17th Brazilian Congress of Thermal Sciences and Engineering
November 25th-28th, 2018, Águas de Lindóia, SP, Brazil

# ENCIT-2018-0741
# THERMODYNAMICS ANALYSIS OF INTERNAL COMBUSTION ENGINES USING QUASI-DIMENSIONAL AND ZERO-DIMENSIONAL MODELS

**Daniel da Silva Tonon - ds.tonon@gmail.com**
**Ezio Castejon Garcia - ezio@ita.br**
Instituto Tecnológico de Aeronáutica – ITA – Divisão de Engenharia Mecânica
Praça Marechal Eduardo Gomes, 50
Vila das Acácias, 12228-900
São José dos Campos/SP – Brasil

***Abstract.*** *Among all the mechanisms that make up a car, the engine deserves a special mention, since it is responsible for power generation and is through it that the vehicle will start your movement. Over time the design of this engine had to evolve considerably compared with the first cars manufactured in the history, because of the social and ecological requirements. In this way,it is of fundamental importance that the automakers to evaluate the behavior of the engine in your whole operating range, and this evaluation can be done through different numerical models. The most widespread models for the simulation of these mechanisms are CFD models, zero-dimensional models and quasi-dimensional models. In this paper is shown a comparative analysis between experimental results and results obtained through simulations of internal combustion engines using quasi-dimensional and zero-dimensional models.*

***Keywords:*** *Internal Combustion Engine, Wiebe Curve, Flame Speed*

## 1. NOMENCLATURE

$T$: temperature
$T_u$: temperature of unburned gases
$T_b$: temperature of the burned gases
$T_{ref}$: reference temperature (297 K)
$T_{wall}$: wall temperature
$T_r$: temperature after admission
$m_{in}$: intake mass
$m_{ex}$: exhaust mass
$m_u$: unburned mass
$m_b$: burned mass
$c_p$: specific heat at constant pressure
$c_{pu}$: specific heat at constant pressure of the unburned mass
$c_{pb}$: specific heat at constant pressure of the burned mass
$Q$: heat transferred
$Q_u$: heat transferred by the unburned mass
$Q_b$: heat transferred by the burned mass
$h_{in}$: enthalpy of mass at intake
$h_{ex}$: enthalpy of mass at exhust
$h_u$: enthalpy of the unburned mass
$h_b$: enthalpy of the burned mass
$V$: total volume
$V_u$: unburned volume
$V_b$: burned volume
$V_r$: pressure after admission
$V_{dt}$: swept volume
$p$: pressure
$p_{ref}$: reference pressure (1 atm)
$p_r$: pressure after admission
$p_m$: motoring pressure
$\rho$: density
$\rho_u$: density of the unburned mass
$\rho_b$: density of the burned mass
$R_u$: gas independent constant for the unburned mass
$R_b$: gas independent constant for the burned mass
$S_L$: laminar flame speed
$S_{L,0}$: reference laminar flame speed
$S_T$: turbulent flame speed
$f$: phenomenological factor
$x_b$: fraction of burned mass
$rot$: speed in revolutions per minute
$y_r$: fraction of burned mass
$\alpha$: exponencial coeficiente
$\beta$: exponencial coeficiente
$\phi$: equivalence ratio
$\phi_m$: equivalence ratio parameter for $S_{L,0}$ maximum
$B_m$: parameter for calculation of $S_{L,0}$
$B_\phi$: parameter for calculation of $S_{L,0}$
$\theta$: crank angle
$\theta_i$: start angle of combustion
$\theta_f$: end-of-combustion angle
$a_{wie}$: wiebe efficiency factor
$m_{wie}$: wiebe form factor
$n$: number of moles of a given species
$N$: number of total mols
$a_s$: number of air moles for stoichiometric combustion
$y$: molar fraction
$K$: equilibrium constant
$h_{wos}$: coefficient of heat transfer
$u$: characteristic speed

*k*: coefficient polytropic

## 2. INTRODUCTION

The use of internal combustion engines to transport people is still a worldwide reality. The first of these mechanisms to have had a patent application dates back to 1854, made by the Italian engineers Eugenio Barsanti and Felice Matteucci (Belli, 2013). However, from that date to the present day, combustion engines have go through major modifications, like in the components used, in the peripherals introduced to assist in certain tasks, or even in their geometry. These modifications are still being introduced for several reasons, most of all the customer's requirements, which wanted to have a vehicle with higher performance and lower consumption. And added to this, we still have environmental restrictions on emissions.

Much of the analysis involving these mechanics is still done in an experimental way, through bench tests using dynamometers. However, this part of the project is extremely costly, since it requires several inputs, such as fuel, data acquisition systems, measuring instruments, electricity, among others. We can say that the process of homologation of an internal combustion engine used in popular vehicles has a cost in the order of millions.

There is then a need to simulate these thermal machines in order to minimize the costs on experimental tests, but this is not an easy task and it would be very naive to believe that an internal combustion engine can be modeled directly by applying relations of the first and second laws of thermodynamics plus the conservation of mass. Of course, these laws and the above-mentioned concepts are extremely important, since they work (isolated) very well for didactic purposes, and from these, we begin to think of a model, but certainly it's not enough for the faithful characterization of an engine.

One way, perhaps, of approaching a more realistic model would be to analyze each of the events that occur during the cycle of an internal combustion engine, in order to consider the many particularities that occur in each event, introducing the losses and imperfections.

However, in the case of an internal combustion engine, it would not be enough to analyze only the events predicted in the thermodynamic cycle, since there are other phenomena that also occur beyond those analyzed, for example the losses that are related to the contacts between connecting rod, crankshaft and bearings, among others, which are not computed when we analyze only what happens inside the combustion chamber.

Fortunately, the technological advances provide us with the possibility of using computational resources to create models that are much more complex and that can compute all the above-mentioned particularities (or even others that go beyond this text), without great difficulties, requiring only that they be well defined.

This paper presents a comparison between Quasi-dimensional and Zero-dimensional models, using the equations described by Curto (2014) for the thermodynamic characterization. All analyzes reported in this text are qualitative, not quantitative, so that the main objective is to be able to reproduce the behavior of the data used.

## 3. ZERO-DIMENSIONAL AND QUASI-DIMENSIONAL MODELS

Zero-Dimensional models, also known as Single-Zone, are numerical models where the only independent variable is time (Curto, 2014). Therefore, these models consider that the composition and thermodynamic properties, such as temperature and pressure, are spatially uniform, and will only vary by the influence of time (Feng, 2014). These types of models generally use an empirical relationship to determine the rate of fuel consumption, or analytical functions, such as the Wiebe curve, which is the empirical equation used for the Zero-dimensional model calculations of this paper.

In Multi-Zone models, the combustion chamber is divided into several regions. Each of these regions can exchange heat and mass with adjacent regions, be it another region of the combustion chamber or the cylinder wall. The temperature of each of these regions is distinct and homogeneous within that region, and of course the pressure for all regions is the same. Figure 1 shows an example of division of the combustion chamber in a Multi-Zone model. The great advantage of these models in relation to the Single-Zone models is that we can verify more complex phenomena, such as temperature stratification, or species within the combustion chamber. These types of information are important in estimating the duration of combustion, and the rate of increase in pressure as the cycle progresses.

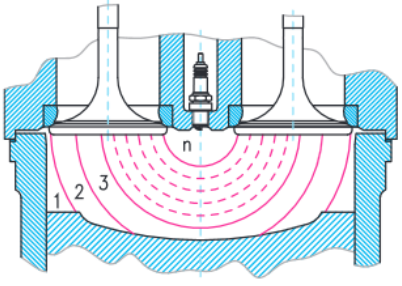


Figure 1. Example of the division of the combustion chamber for a Multi-Zone model with n regions (Hvezda, 2012).

In the case of this text, however, a particular case of the Multi-Zone models, which are the Quasi-Dimensional models, is used. They divide the combustion chamber into only two regions, and only during the combustion event. It is assumed that during combustion the flame will propagate in a spherical way, filling the volume of the combustion chamber until there are no more species to be oxidized in the chamber. The way to determine the evolution of this spherical cap can be made using analytical equations, such as the Wiebe curve, or with the aid of a submodel that determines the velocity of flame propagation. The Quasi-Dimensional type model proposed in this work uses a submodel for calculating the flame speed.

Other types of model that can be mentioned as an alternative to the simulation of Internal Combustion Engines are the Multi-Dimensional models, which are strongly associated with CFD analysis, but these are not very used for the determination of parameters such as torque and power, since they require a much longer calculation time than the previously described models. These analyzes are most often used in specific cases, such as determining the temperature of the exhaust valve seat, for example.

## 4. METHODOLOGY

The development of the equation will not be demonstrated in this paper, but can be found in Curto (2014). Here only the main equations used to obtain the Temperature and Pressure will be shown.

The temperature change rate is obtained through Eq. (1):

$$\dot{T} = \frac{1}{(m_u \cdot c_{p,u} + m_b \cdot c_{p,b})} \cdot [\dot{Q}_u + \dot{Q}_b + \dot{m}_{in} \cdot h_{in} - \dot{m}_u \cdot h_u + \dot{m}_{ex} \cdot h_{ex} - \dot{m}_b \cdot h_b + V \cdot \dot{p}] \tag{1}$$

And the Pressure change rate is obtained with the Eq. (2):

$$\dot{p} = \left[p \cdot \left(\frac{\dot{m}_u}{\rho_u} + \frac{\dot{m}_b}{\rho_b} - \dot{V}\right) + \zeta \cdot \left(\dot{Q}_u + \dot{Q}_b + \dot{m}_{in} \cdot h_{in} - \dot{m}_u \cdot h_u + \dot{m}_{ex} \cdot h_{ex} - \dot{m}_b \cdot h_b\right)\right] \cdot \frac{1}{[V \cdot (1 - \zeta)]} \tag{2}$$

Being:

$$\zeta = \frac{V}{\frac{V_u \cdot c_{p,u}}{R_u} + \frac{V_b \cdot c_{p,b}}{R_b}} \tag{3}$$

Of course, not all cycle events will need all of these parameters present in equations (1), (2) and (3). Note that during the intake event the exhaust valve will be closed, and therefore there will be no mass coming out of the control volume, then that term will be zero. In addition, during admission, the mass rate entering the control volume will be equal to the unburned mass rate in the control volume. The same type of argument can be extended to the event of exhaustion. Note also that during compression and motor expansion, the combustion chamber will be a closed system, so that all terms referring to the mass inlets and outlets will be zero.

### 4.1 Quasi-Dimensional Combustion

For this submodel it is assumed that as soon as the spark plug is started, the combustion starts at the point where the spark is generated, and so the flame front will propagate throughout the combustion chamber with the shape of a spherical cap. Figure 2 represents this type of behavior.

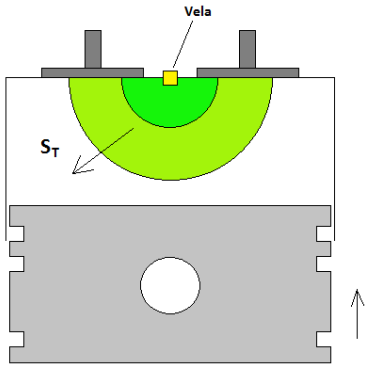


Figure 2. Representation of the flame propagation by the combustion chamber.

As shown in Fig. 2, the flame propagates with an intensity equal to the velocity of turbulent flame front propagation, relative to the fuel and the thermodynamic conditions within the combustion chamber, for each instant. The following correlation (Curto, 2014), proposes the calculation of the turbulent flame speed to be proportional to the the laminar flame speed:

$$S_T = f \cdot S_L \cdot \frac{\frac{\rho_u}{\rho_b}}{\left(\frac{\rho_u}{\rho_b} - 1\right) \cdot x_b + 1} \tag{4}$$

The phenomenological factor, $f$ (Curto, 2014), present in Eq. (4), is calculated as follows:

$$f = 1 + 0{,}0018 \cdot rot \tag{5}$$

For the calculation of laminar flame speed, is used the Kerk correlation, described in Heywood (1988):

$$S_L = S_{L,0} \cdot \left(\frac{T_u}{T_{ref}}\right)^{\alpha} \cdot \left(\frac{p}{p_{ref}}\right)^{\beta} \cdot (1 - 2{,}06 \cdot y_r^{0{,}77}) \tag{6}$$

The coefficients $\alpha$, $\beta$ e $S_{L,0}$, are obtained as follows:

$$\alpha = 2{,}18 - 0{,}8 \cdot (\phi - 1) \tag{7}$$

$$\beta = -0{,}16 + 0{,}22 \cdot (\phi - 1) \tag{8}$$

$$S_{L,0} = B_m + B_\phi \cdot (\phi - \phi_m)^2 \tag{9}$$

### 4.2 Zero-dimensional combustion

In Zero-Dimensional models, as mentioned before, the only independent variable is time, so that combustion must be modeled from an empirical equation. In the case of this paper, the empirical equation used was the Wiebe curve (Ferguson, 2001), shown in Eq. (10).

$$x_b(\theta) = 1 - \exp\left[-a_{wie} \cdot \left(\frac{\theta - \theta_i}{\theta_f - \theta_i}\right)^{m_{wie}+1}\right] \tag{10}$$

Another relation that could be used is the as called cosine function, but the Wiebe's curve is more commonly used in scientific work because it has a greater precision in the results (Caton, 2016).

### 4.3 Chemical reactions

During combustion, the air and fuel mixture will go through an oxidation process, and then this mixture will be converted into other species that will be called combustion products. The number of species and intermediate reactions during this process is extensive, becoming impracticable for the analyzes proposed by the presented model.

In this way, a simpler chemical reaction model is adopted, but sufficient for the desired analyzes. This model is described in Ferguson (2001), and considers the global reaction, with the formation of the following species:

$$C_\alpha H_\beta O_\gamma N_\delta + \frac{a_s}{\phi}(O_2 + 3{,}76N_2) \rightarrow n_1 CO_2 + n_2 H_2O + n_3 N_2 + n_4\, O_2 + n_5\, CO + n_6\, H_2 + n_7 H + n_8\, O + n_9\, OH + n_{10}\, NO \tag{11}$$

It is therefore necessary to find the number of moles of each species. Through the chemical balance of the components:

$$C: \alpha = (y_1 + y_5) \cdot N \tag{12}$$

$$H: \beta = (2 \cdot y_2 + 2 \cdot y_6 + y_7 + y_9) \cdot N \tag{13}$$

$$O: \gamma + \frac{2 \cdot a_s}{\phi} = (2 \cdot y_1 + y_2 + 2 \cdot y_4 + y_5 + y_8 + y_9 + y_{10}) \cdot N \tag{14}$$

$$N: \delta + \frac{3{,}76 \cdot a_s}{\phi} = (2 \cdot y_3 + y_{10}) \cdot N \tag{15}$$

It is also known that:

$$\left(\sum_{i=1}^{10} y_i\right) - 1 = 0 \tag{16}$$

However, there are 11 unknowns (the molar fractions of each component plus the total number of moles), and only 5 equations. The other six equations are given from the equilibrium constants of some reactions, which are:

$$\frac{1}{2} \cdot H_2 \Leftrightarrow H \qquad K_1 = \frac{y_7 \cdot p^{0,5}}{y_6^{0,5}} \tag{17}$$

$$\frac{1}{2} \cdot O_2 \Leftrightarrow O \qquad K_2 = \frac{y_8 \cdot p^{0,5}}{y_4^{0,5}} \tag{18}$$

$$\frac{1}{2} \cdot O_2 + \frac{1}{2} \cdot H_2 \Leftrightarrow OH \qquad K_3 = \frac{y_7}{y_4^{0,5} \cdot y_6^{0,5}} \tag{19}$$

$$\frac{1}{2} \cdot O_2 + \frac{1}{2} \cdot N_2 \Leftrightarrow NO \qquad K_4 = \frac{y_{10}}{y_4^{0,5} \cdot y_3^{0,5}} \tag{20}$$

$$\frac{1}{2} \cdot O_2 + H_2 \Leftrightarrow H_2O \qquad K_5 = \frac{y_2}{y_4^{0,5} \cdot y_6 \cdot p^{0,5}} \tag{21}$$

$$\frac{1}{2} \cdot O_2 + CO \Leftrightarrow CO_2 \qquad K_6 = \frac{y_1}{y_4^{0,5} \cdot y_5 \cdot p^{0,5}} \tag{22}$$

The value of each of these constants is obtained through the following correlation:

$$\log_{10} K_i(T) = A_i \cdot \ln\left(\frac{T}{1000}\right) + \frac{B_i}{T} + C_i + D_i \cdot T + E_i \cdot T^2 \tag{23}$$

The values of $A_i$, $B_i$, $C_i$, $D_i$ e $E_i$ for each of the constants are given in Ferguson (2001).

### 4.4 Thermal Exchanges

In general, for the estimation of heat exchanges, two models are more widespread, being the models proposed by Annand (1970-1971) and Woschni (1967). The first attempts to characterize heat exchanges in general, in other words, including all mechanisms of heat exchange during the cycle. The second model (Woschni), which is also widely used, unlike the previous model, does not consider radiation losses as part of the equation, but adds the contribution of this mechanism indirectly.

Here we chose to work with the Woschni model, which is based on the following equation:

$$\dot{q} = h_{wos} \cdot (T - T_{wall}) \tag{24}$$

Since the global heat transfer coefficient is obtained through the following correlation:

$$h_{wos} = 129{,}8 \cdot p^{08} \cdot D^{-0,2} \cdot T^{-0,53} \cdot u^{0,8} \tag{25}$$

The characteristic speed is calculated as follows:

$$u(t) = C_1 \cdot v_p + C_2 \cdot \frac{V_{dt} \cdot T_r}{p_r \cdot V_r} \cdot [p(t) - p_m] \tag{26}$$

Being that the pressure, temperature and reference volume are the values of these properties at the time the inlet valve is closed. The coefficients $C_1$ and $C_2$ have different values for each event of the cycle and these values can be consulted in Curto (2014). The motoring pressure, $p_m$, can be calculated by a polytropic ratio:

$$p_m = p_r \cdot \left(\frac{V_r}{V}\right)^k \tag{27}$$

## 5. RESULTS AND DISCUSSION

In this part of the text will be presented some results obtained with the proposed models. It should be remembered that the objective is not to achieve high precision of the results obtained with the models in relation or experimental data, but is wanted to represent the behavior of the phenomenon, so that these models can be further improved. All data analyzed refer to 4-stroke engines.

Figure 3 compares the proposed models with experimental data of a 4-cylinder in-line engine, total displaced volume of 1581 cm³, compression ratio of 9.2, diameter of 86.4 mm, stroke of 67.4 mm, equivalence ratio 1.11, speed of 3000 rpm and in full load condition. These experimental data were obtained from Millo (2013). It is observed that the results obtained with the models represent with great fidelity the experimental data, presenting few disagreements and reproducing the behavior observed in the tests, however, it is noticed that there are differences between the results obtained between the models. For the curve obtained with the Quasi-Dimensional model, the mean deviation from the experimental data is 2.5%, where as for the Zero-Dimensional model, this deviation is 3.5%.

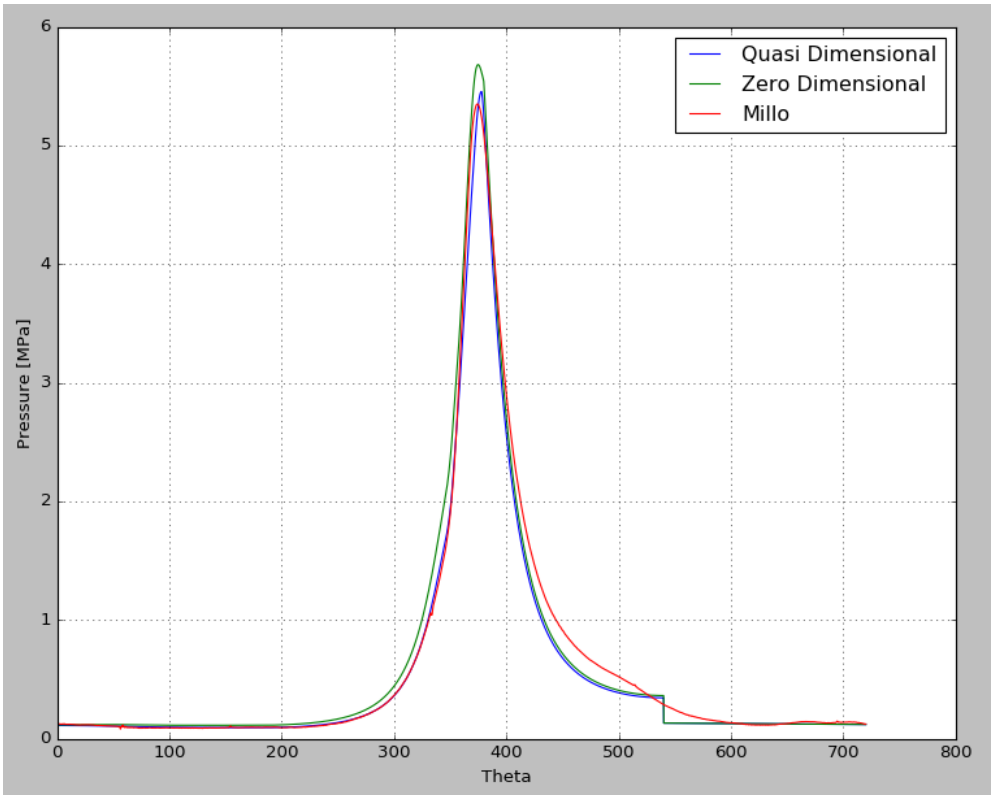


Figura 3. Comparison of Millo's data (2013) with simulated results.

Figure 4 compares the proposed models with experimental data of an engine with compression ratio 9.4, diameter 72 mm, stroke of 61 mm, equivalence ratio 1, speed of 1500 rpm and under minimum load condition. The experimental data were obtained from Chitragar (2015). In this case the results of the models distance themselves from the experimental ones, but still it is noticed that the behavior is maintained, as well as the peak of pressure of the cycle. The observed mean deviations for these results are 15.5% for the Quasi-Dimensional model and 14.3% for the Zero-Dimensional model.

These deviations can be considered high, but again, it is important to notice that the intention of this work is to represent the behavior of the cycle initially.

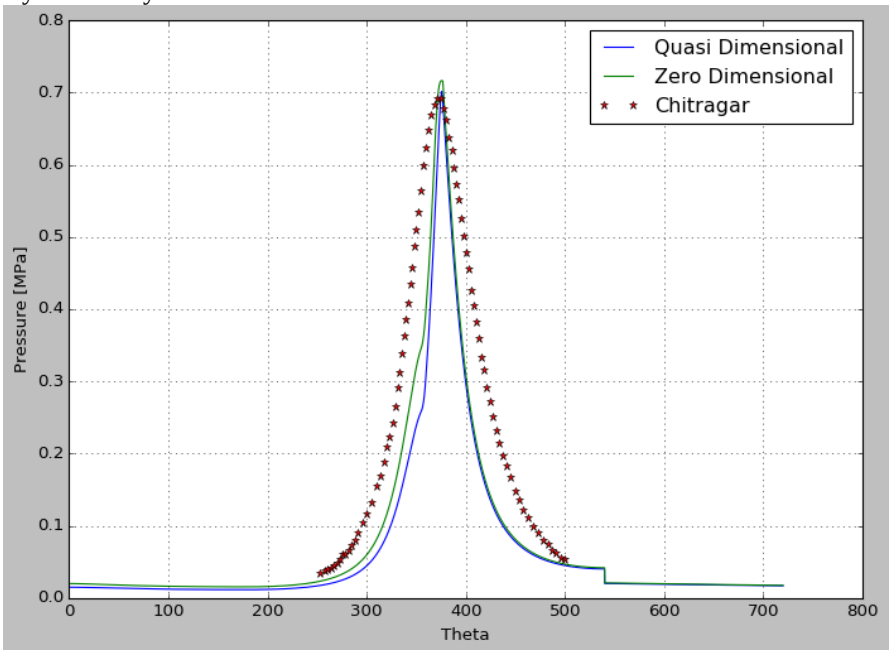


Figura 4. Comparison of Chitragar (2015) data with simulated results.

Figure 5 compares the proposed models with experimental data of an engine with compression ratio 10, diameter 77.4 mm, stroke 85 mm, equivalence ratio 1, ignition point 26 degrees before PMS, speed of 1400 rpm and a pressure in the intake manifold of 61.5 kPa. The experimental data were obtained from Ji (2016). In this case, the results of the model are lagged from the experimental data, but it can be considered that the results represent the observed behavior in practice. The observed mean deviations are approximately 6.5% for both models, however, when considering the area below the curve, these deviations are smaller.

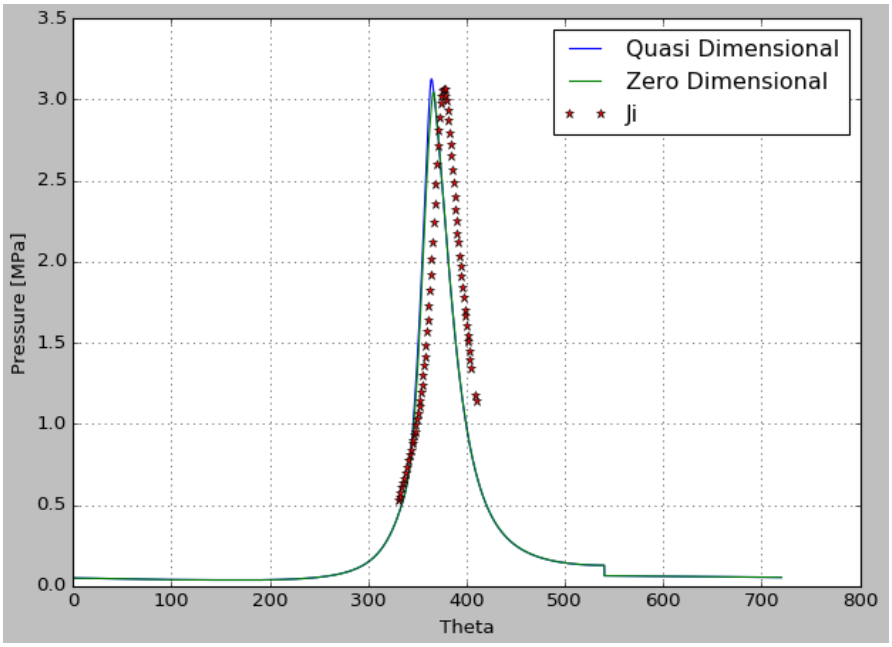


Figura 5. Comparison of Ji (2016) data with simulated results.

Figure 6 compares the proposed models with experimental data of an engine with compression ratio 10, diameter 77.4 mm, stroke 85 mm, equivalence ratio 0.79, ignition point 22 degrees before PMS , a speed of 1400 rpm and a pressure in the intake manifold of 61.5 kPa. The experimental data were obtained from Martínez (2016). The average deviations are 9% for the Quasi-Dimensional model and approximately 12% for the Zero-Dimensional model, which again are high, but

it is noted that the two models represent well the behavior of the experimental data, presenting some differences between the maximum pressure value reached and a slight lag in relation to the experimental results.

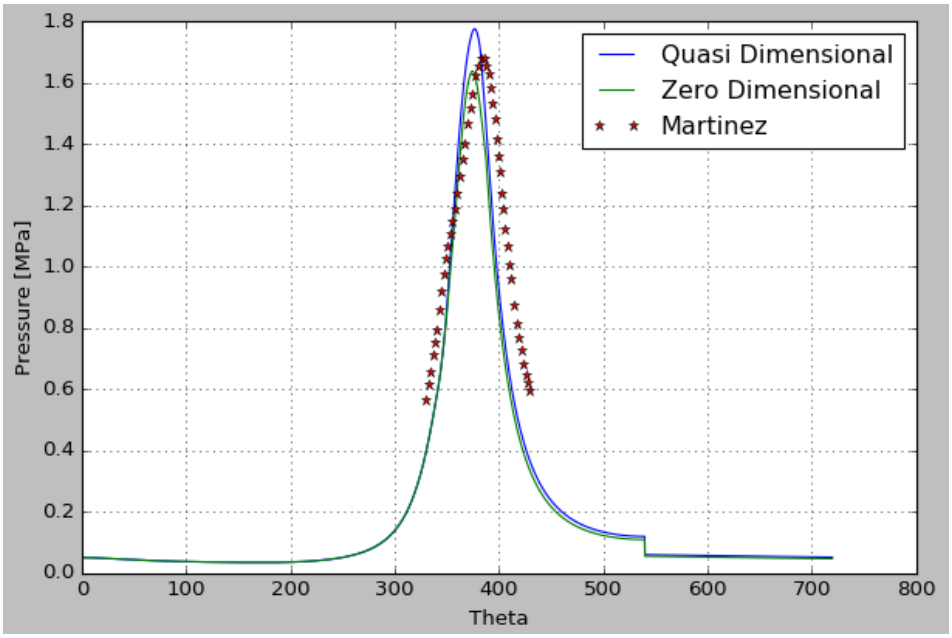


Figura 6. Comparison of data from Matinez (2016) with simulated results.

Finally, Figure 7 compares the proposed models with experimental data of an engine with compression ratio of 9.5, 81 mm diameter, stroke of 89 mm, equivalence ratio 1, ignition point of 20 degrees before PMS, speed of 3500 rpm and a pressure in the intake manifold of 50 kPa. The experimental data were obtained from Yusri (2016). The deviations for both models were approximately 19%, which again are high, however, it is noted that the peak pressure was well represented, as well as the behavior of the cycle.

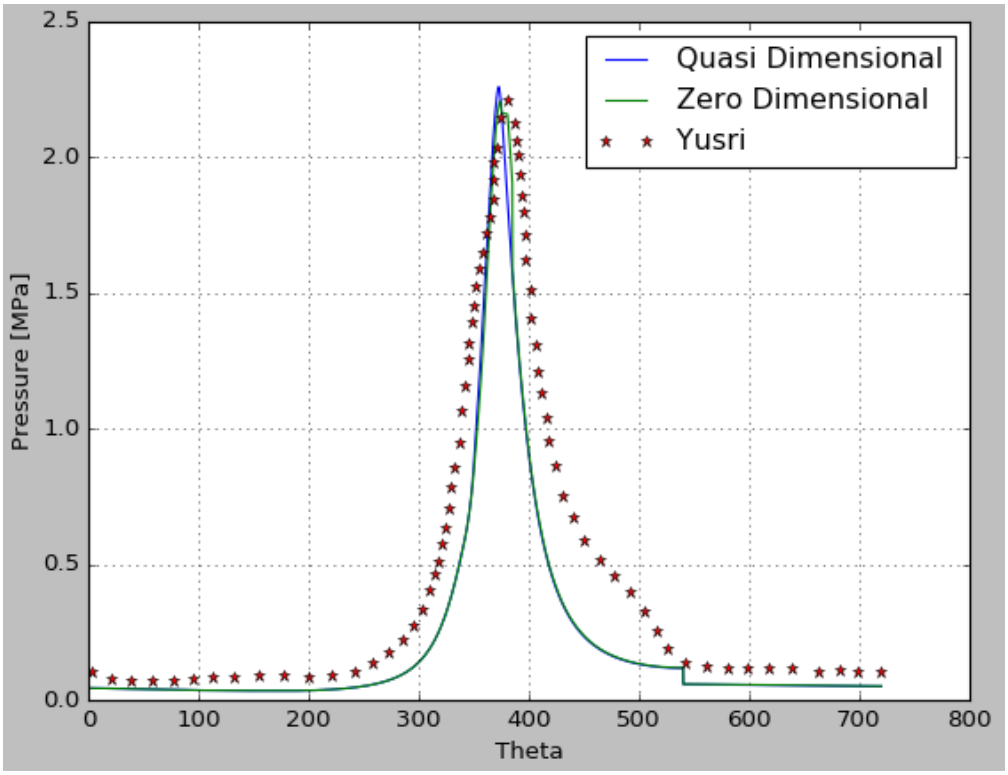


Figura 7: Comparison of Yusri's data (2016) with simulated results.

## 6. CONCLUSIONS

The models presented in this paper show great potential for the performance analysis of internal combustion engines. Due to the fact that these codes are still not very refined, the results are considered satisfactory, and the main objective was reached, since it is possible to represent the behavior of real cases.

When comparing the results obtained by both models, no significant differences were observed, and the two models represent the behavior of the thermal machine in a similar way. There were also no differences between the models as to the time required for the simulations, which was an unexpected result, since the number of equations of the Quasi-Dimensional model during the combustion analysis is much higher than the Zero-Dimensional model.

The observed deviations in the presented results are probably related to the limitations of the models regarding the gas exchanges, being that they were modeled disregarding effects of overlap and lift of the valves, which may be generating a difference in the mass of air admitted per cycle. Unfortunately, the data concerning the mass allowed for the simulated conditions were not available, making this analysis impossible, however, new gas exchange models will be implemented in future versions of the codes.

In addition to a more appropriate model for gas exchange, it is planned for future work the insertion of more sophisticated models for the representation of friction and emissions.

## 7. REFERENCES

Annand, W. J. D. et al., 1970-1971. "Instantaneous Heat Transfer Rates to the Cylinder Head Surfece of a Small Compression-Ignition Engine". *Proc. Inst. Mech. Engrs*, Vol. 185, p. 976-987.

Belli, M., 2013. "Motores de combustão interna, uma breve História". 5 Aug. 2017 <http://www.autoentusiastasclassic.com.br/2013/03/motores-combustao-interna-uma-breve.html >.

Caton, J. A., 2016. *An introduction to thermodynamic cycle simulation for internal combustion engines*. John Wiley & Sons, West Sussex.

Chitragar, P. R. et al., 2015. "An experimental study on combustion and emission analysis of four cylinder 4-stroke gasoline engine using pure hydrogen and LPG at idle condition". *Energy Procedia*, Vol. 90, p. 525-534.

Curto-Risso, P. L. et al., 2014. *Quasi-Dimensional Simulation of Spark Ignition Engines.* Springer, London.

Feng, H. et al., 2014. "Availability analysis of n-heptane/iso-octane blends during low-temperature engine combustion using a single-zone combustion model". *Energy Conversion and Management*, Vol. 84, p. 613-622.

Ferguson, C. R. and Kirkpatrick, A. T., 2001. *Internal Combustion Engines Apllied Thermosciences*. John Wiley & Sons, New York, 2nd edition.

Heywood, J. B., 1988. *Internal Combustion Engine Fundamentals.* McGraq-Hill Book Company, New York.

Hvezda, J., 2012. "Multi-Zone Models of Combustion and Heat Transfer Processes in SI Engines". *Journal of Middle European Construction and Design of Cars*, 10.2478/v10138-012-0008-6, p. 14-22.

Ji, C. et al., 2016. "A quasi-dimensional model for combustion performance prediction of an SI hydrogen-enriched methanol engine". *Hydrogen Energy*, Vol. 41, p. 17676-17686.

Martínez-Boggio, S. D. et al., 2016. "Simulation of cycle-to-cycle variations on spark ignition engines fueled with gasoline-hydrogen blends". *Hydrogen Energy*, Vol. 41, p. 9087-9099.

Millo, F., 2013. *Esercitazione Volano*. Publicação Interna - Politecnico di Torino, Turin.

Woschni, G., 1967. "Universally Applicable Equation for the Instantaneous Heat Transfer Coefficient in the Internal Combustion Engine". *SAE paper*, Vol. 76, n. 670931.

Yusri, I. M. et al., 2016. "Experimental investigation of combustion, emissions and thermal balance of secondary butyl alcohol-gasoline blends in a spark ignition engine". *Energy Conversion and Management*, Vol. 123, p. 1-14.

## 8. RESPONSIBILITY NOTICE

The authors are the only responsible for the printed material included in this paper.